

The PanAf-FGBG Dataset: Understanding the Impact of Backgrounds in Wildlife Behaviour Recognition

Otto Brookes^{1,2†*}, Maksim Kukushkin^{3,4*}, Majid Mirmehdi¹, Colleen Stephens⁵, Paula Dieguez⁵,
Thurston C. Hicks⁶, Sorrel Jones⁵, Kevin Lee⁵, Maureen S. McCarthy⁵, Amelia Meier⁵,
Emmanuelle Normand², Erin G. Wessling⁷, Roman M. Wittig^{5,8}, Kevin Langergraber⁹,
Klaus Zuberbühler¹⁰, Lukas Boesch², Thomas Schmid^{4,11}, Mimi Arandjelovic⁵,
Hjalmar Kühl^{5,12}, Tilo Burghardt¹

¹University of Bristol, ²Wild Chimpanzee Foundation, ³Leipzig University,

⁴Martin Luther University Halle-Wittenberg, ⁵Max Planck Institute for Evolutionary Anthropology,

⁶University of Warsaw, ⁷Harvard University, ⁸University of Lyon, ⁹Arizona State University,

¹⁰University of St Andrews, ¹¹Lancaster University in Leipzig, ¹²Senckenberg Museum of Natural History

Abstract

Computer vision analysis of camera trap video footage is essential for wildlife conservation, as captured behaviours offer some of the earliest indicators of changes in population health. Recently, several high-impact animal behaviour datasets and methods have been introduced to encourage their use; however, the role of behaviour-correlated background information and its significant effect on out-of-distribution generalisation remain unexplored. In response, we present the PanAf-FGBG dataset, featuring 20 hours of wild chimpanzee behaviours, recorded at over 350 individual camera locations. Uniquely, it pairs every video with a chimpanzee (referred to as a foreground video) with a corresponding background video (with no chimpanzee) from the same camera location. We present two views of the dataset: one with overlapping camera locations and one with disjoint locations. This setup enables, for the first time, direct evaluation of in-distribution and out-of-distribution conditions, and for the impact of backgrounds on behaviour recognition models to be quantified. All clips come with rich behavioural annotations and metadata including unique camera IDs and detailed textual scene descriptions. Additionally, we establish several baselines and present a highly effective latent-space normalisation technique that boosts out-of-distribution performance by +5.42% mAP for convolutional and +3.75% mAP for transformer-based models. Finally, we provide an in-depth analysis on the role of backgrounds in out-of-distribution behaviour recognition, including the so far unexplored impact of background durations (i.e., the count of background frames within foreground videos).

1. Introduction

Deep learning models have shown impressive results on action recognition tasks [47], particularly when both training and test data share the same distribution. However, their performance declines significantly on out-of-distribution (OOD) data [11, 23]. In practice, distribution shifts are common in nearly *all* settings [36], but are particularly unforgiving when computer vision is applied to uncontrolled, complex or natural environments [23].

In the human action recognition domain, poor OOD performance is well-known to originate from shortcut learning [14] of static cues or backgrounds [20, 25, 26]. This leads models to rely heavily on background information instead of the behaviour of interest, and several studies have shown that the *majority* of action recognition performance in this domain can be attributed to background learning [8, 18, 41]. Despite the known impact of backgrounds on action recognition and a critical need to advance model performance in challenging wildlife applications [24, 40], reliance on static cues for animal behaviour recognition has received only limited attention. This is largely due to a lack of datasets explicitly designed to study its effects.

In response, we introduce the PanAf-FGBG dataset, which comprises real-world foreground-background video pairs (see Fig. 1) extracted from six African countries, 14 national parks, and over 350 individual camera locations across many habitats and location types (see Fig. 3). Here, we define foreground videos as those containing a chimpanzee, and background videos as those that do not. This allows us to address a key limitation in existing studies, where the background’s role is typically assessed by creating background-only versions of datasets through synthetic modifications (e.g., masking or in-painting) that remove the actor [7, 8, 19]. While such synthetic inputs often serve as useful proxies, the actual effect of synthesis on training is

†Corresponding author, *Equal technical contribution



Figure 1. **Conceptual Overview.** The PanAf-FGBG dataset comprises 20+ hours of paired and richly annotated foreground-background videos from camera traps in wild chimpanzee habitats (see example frames at the top). The dataset unlocks systematic analyses of the impact of background information on wildlife behaviour recognition. We provide baselines, quantify the background impact in relation to other sources of information, and demonstrate that utilising background information in latent space (see blue data point) can significantly improve recognition performance in this challenging domain.

largely unknown [34, 39].

In contrast, our dataset introduces paired camera locations and enables a truly realistic disentangling of background effects under in- and out-of-distribution conditions: *disjoint* experiments with mutually exclusive camera locations for training and test splits, and *overlapping* experiments with shared locations. This focus is particularly important in the wildlife domain, where the transferability and generalisation of camera trap analysis to new locations is critical for effective operation. While studies have shown the over-reliance of action recognition models on backgrounds [18, 32, 41], we find that the effect of *background duration* (i.e., the count of background frames within foreground videos with no actor) is largely unexplored. In camera trap video footage like in many other CCTV or triggered

camera settings, actors may only appear momentarily, leaving behind footage of *only* the background [10, 33] within foreground videos. Since this effect alters learning given video-level behaviour annotations, we quantify its effect on several action recognition architectures.

Our contributions are as follows: (i) we release PanAf-FGBG with its rich annotations and meta-data, providing a large wildlife dataset suitable for explicitly investigating the impact of backgrounds on behaviour recognition; (ii) we show models trained on background-only videos achieve strong animal behaviour recognition performance ($\sim 65\%$ of baseline performance), corroborating findings in the human domain; (iii) we conduct the first evaluation of background duration in videos, revealing its impact on action recognition models and highlighting key differences between convolutional and attention-based networks; and (iv) we introduce a simple yet powerful latent-space background neutralisation that yields notable performance gains, particularly in OOD scenarios for both convolutional (+5.42% mAP) and transformer-based approaches (+3.75% mAP).

2. Related Work

Animal Behaviour Datasets. In recent years, several high-impact animal behaviour datasets have been introduced to the CV community [4, 6, 22, 29, 31, 35]. Although they all centre on animal behaviour understanding, they each have a different focus. The large-scale datasets Animal Kingdom [35] and MammalNet [6] focus on behavioural understanding across species, each including videos of ~ 800 different species. They provide atomic action and high-level behaviour annotations, respectively, and support, in addition to action recognition, the related tasks of action localisation [6, 35] and pose estimation [35]. The smaller ChimpAct dataset [31] provides longitudinal data that follows a zoo-housed group of 20 chimpanzees with a focus on a single male juvenile. It also contains key-point pose information, and fine-grained spatio-temporal behaviour labels. While valuable, these datasets lack in-situ footage from ecological sensors like camera traps and drones, meaning animals are not observed in their natural environment. This may result in unrepresentative behaviour distributions and limit their suitability for studying wild behaviour [5, 9].

In contrast, KABR [22] and BaboonLand [13] comprise drone footage of free-living Kenyan wildlife, with fine-grained spatio-temporal behaviour annotations, focussing on individual and group-level behaviour, respectively. The LoTE dataset [29] provides camera trap video footage of 11 endangered species from a 12-year longitudinal study; it is accompanied by environmental information (i.e., weather conditions and habitat) and highlights the importance of temporal and spatial continuity for conservation efforts. The dataset most comparable to our own is the PanAf20k

dataset [4], which comprises camera trap videos of great apes accompanied by multi-label behaviour annotations.

Our dataset orthogonally complements the growing body of work dedicated to understanding animal behaviour by providing the first dataset specifically designed to evaluate backgrounds and out-of-distribution generalisation for behaviour recognition. It is unique in providing foreground-background pairs, and its configurations for in- and out-of-distribution evaluation are defined identically to the well-known iWildCam [3] and Wilds dataset [23] for species classification. Similar to LotE [29], we provide a detailed description of the background, however we also include a unique camera ID (i.e., geospatial location) to allow footage taken from the same camera to be linked. Similar to [4], our data is gathered from 14 national parks, spanning 6 different countries, although unlike ours they do not include metadata to allow videos to be linked to specific countries, research sites, locations, or habitats. Similarly, it is more diverse than [29] with its footage from a single national park.

Background Impact. The effect of backgrounds or static bias is well-studied within computer vision [25, 44], where it has shown to be *necessary* for models to perform well [43]. Action recognition models are particularly vulnerable to shortcut learning. These models often rely on correlated, but distinct information beyond the intended action, such as object [16, 46], scene [32], and actor biases [27]. For example, several studies have reported that strong performance on action recognition tasks can be achieved *without* the actor [18, 32, 41] and that approximately 70% of model performance is attributable to static cues (i.e., scene or background) [8]. This results in biased representations and ultimately impairs out-of-distribution generalization performance [26].

Background Bias Datasets. The effect of the background has often been modelled using synthetically generated data that removes either the foreground or the background. [7, 8, 15, 25]. For instance, Ilic et al. [20] present an synthetic version of the UCF101 dataset, animating spatial noise using image motion extracted by an optical flow estimator, Li et al. [25] replace the backgrounds of IID HMDB51 with sinusoidal stripe images, and Chung et al [8] adopt an in-painting model to remove actors from the video. Datasets that include fine-grained spatio-temporal action annotations also remove static cues implicitly by isolating the region of the video where the action is occurring.

Mitigating Background Bias. Prominent attempts to mitigate this bias include dataset resampling methods, which down-weight biased samples [26, 27], adversarial training regimes that rely on scene labels and human masks [7], and augmentation techniques that mix or swap the backgrounds of different videos during training [12, 25, 42]. There are also several implicit approaches, such as frame selection, that aim to utilise only frames where ac-

tivity is occurring [45]. Our dataset, introduced next, instead introduces foreground-background pairing information with close proximity in time of capture, which describes the environment truly independently and in relation to the presence of animals showcasing behaviour.

3. Dataset

Dataset Overview and Statistics. PanAf-FGBG comprises footage gathered under ethical oversight as part of the The PanAf Programme: The Cultured Chimpanzee [1]. It contains 21 hours of camera trap footage of individual chimpanzees in tropical Africa. Its footage is collected from 389 individual camera locations across 14 national parks in 6 African countries. In total, we provide 5,070 video pairs, each 15-seconds in duration. All videos are accompanied by a multi-label behaviour annotation and scene metadata, plus the unique feature of foreground-background video pairing (see Fig. 1). Class and habitat distributions of the data are given in Fig. 2 and Fig. 3, respectively. Our dataset follows a long-tailed distribution common in animal behaviour datasets [4, 6, 29, 31, 35]. The three of the most commonly occurring classes are observed in >60% of videos, while the rarest are observed in fewer than < 3%.

Data Collection. The data collection strategy was designed specifically to maximise the chance of filming the terrestrial activity of apes and we provide only a brief description here (for full details we refer the reader to [1]). Data was collected from 14 different research sites, where an average of 29 movement-triggered Bushnell cameras were installed per site. Grids comprising 20 to 96 1 × 1 km cells were established and one camera was installed per grid cell. Footage was recorded at 30 frames-per-second and a resolution of 1280 × 720. The cameras were visited every 1-3 months for maintenance and to download the recorded footage throughout the study periods.

Ethical Considerations. Both GPS location and habitat

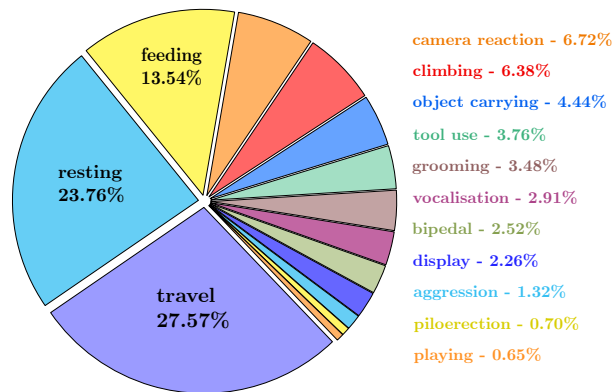


Figure 2. **Distribution of Behaviour.** Proportion of behaviours in the dataset where smaller segments are colour coordinated.

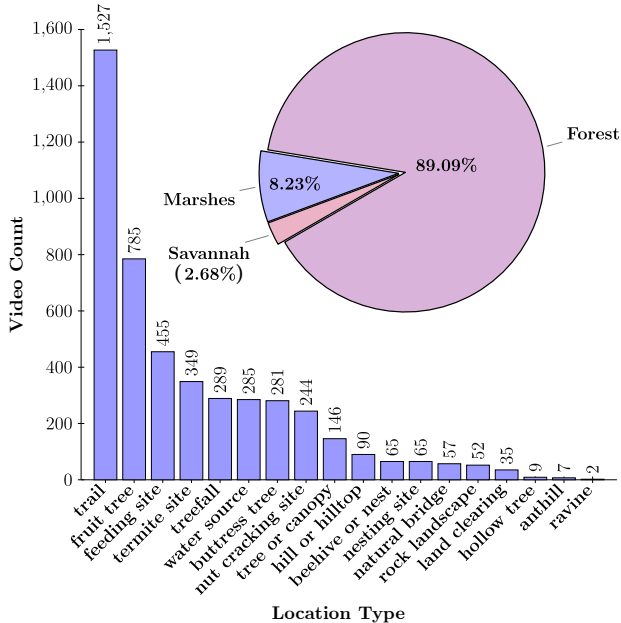


Figure 3. **Distribution of Habitat and Location Type.** The pie chart gives the proportion of videos taken at each of the three main habitats: forest, marshes and savannah. The histogram shows the total number of videos extracted from each location type.

type for each camera was noted during this process. To protect the location of the apes from threats, such as poaching, we use randomly generated monikers for the names of the research sites and assign a unique camera ID to each video, instead of revealing the geospatial location of the cameras.

Data Annotation. The behavioural annotations were provided by users on the community science platform Chimp&See [2]. Annotators were presented with a choice of behaviour classification categories, chosen specifically by experts for their ecological importance. Behaviours not listed in the classification categories were also permitted. These annotations were then extracted and expertly grouped into 14 co-occurring classes, which form the multi-label behavioural annotations presented here. The annotations follow a multi-hot binary format that indicate the presence of one or more behaviours. It should also be noted that behaviours are not assigned to individual apes or temporally localised within each video. To ensure annotation quality and consistency a video was only deemed to be analysed when either three volunteers marked the video as blank, or unanimous agreement between seven volunteers was observed, or 15 volunteers annotated the video.

Overlapping & Disjoint Configurations. We present both a *disjoint* view of dataset, where camera locations in the training and test splits are mutually exclusive, denoted as $\mathcal{D}^{disjoint} = \{d_i \mid d_i \cap d_j = \emptyset, \forall i \neq j\}$ following [23]. A second, *overlapping* view is also provided, where camera

locations are shared between training and test splits, represented as $\mathcal{D}^{overlap} = \{d_i \mid d_i \cap d_j \neq \emptyset \text{ for some } i \neq j\}$. Note that d_i refer to sets of camera locations associated with videos in each split. Fig. 4 provides an overview of both configurations. We ensure that the class distribution in each configuration remains approximately the same for full comparability. Unique camera identifiers are available for each video to allow researchers interested in this problem to create additional configurations, should they wish to.

4. Preliminaries

We train multi-label classification models on both views of the dataset: $\mathcal{D}^{overlap}$ and $\mathcal{D}^{disjoint}$ using various combinations of foreground (\mathcal{F}), background (\mathcal{B}) and synthetic background ($\hat{\mathcal{B}}$) videos. The latter were created by generating a segmentation mask using SAM2 [37] followed by mean pixel value filling, similar to [7, 8, 19]. Both views are comprised of foreground-background video pairs $\{(v_i^{\mathcal{F}}, v_i^{\mathcal{B}})\}_{i=1}^N$, where $v_i^{\mathcal{F}} \in \mathcal{F}$ and $v_i^{\mathcal{B}} \in \mathcal{B}$, with N representing the total number of video pairs. Each foreground video $v_i^{\mathcal{F}}$ is associated with a video-level label vector $y_i = (y_{i1}, y_{i2}, \dots, y_{iC})$, where each $y_{ij} \in \{0, 1\}$ indicates the presence (1) or absence (0) of the j -th class in video i , and C is the total number of classes.

5. Experiments

5.1. Setup

All experiments were performed using the ResNet-50 [17] and MVit-V2 [28] architectures, which were initialised with feature extractors pre-trained on Kinetics-400 [21]. For ResNet-50, both 2D and 3D convolution versions are tested. After initial experiments to ensure optimal optimiser-network pairings for the task, ResNet and MVit-V2 models were fine-tuned for 300 epochs using the SGD [38] and AdamW [30] optimisers, respectively. Both models followed a linear warm-up schedule followed by cosine annealing. For ResNet models, the learning rate was increased from 1×10^{-5} to 1×10^{-4} over 20 epochs, while it was increased from 1×10^{-6} to 1×10^{-4} over 30 epochs for MVit-V2 models. In both cases, momentum of 0.9 was utilised. All computation was performed on 4xNVIDIA H200 GPUs using a distributed batch size of 336. During training, video tensors with a spatio-temporal resolution of $16 \times 256 \times 256$ were employed. Frames were sampled uniformly at a rate of 1/24, avoiding dense sampling strategies which are shown to exacerbate shortcut learning in action recognition models [8]. For MVit-V2 models, a patch size of 16×16 pixels was utilised. Evaluation was performed using micro and mean Average Precision and are referred to as uAP and mAP, respectively.

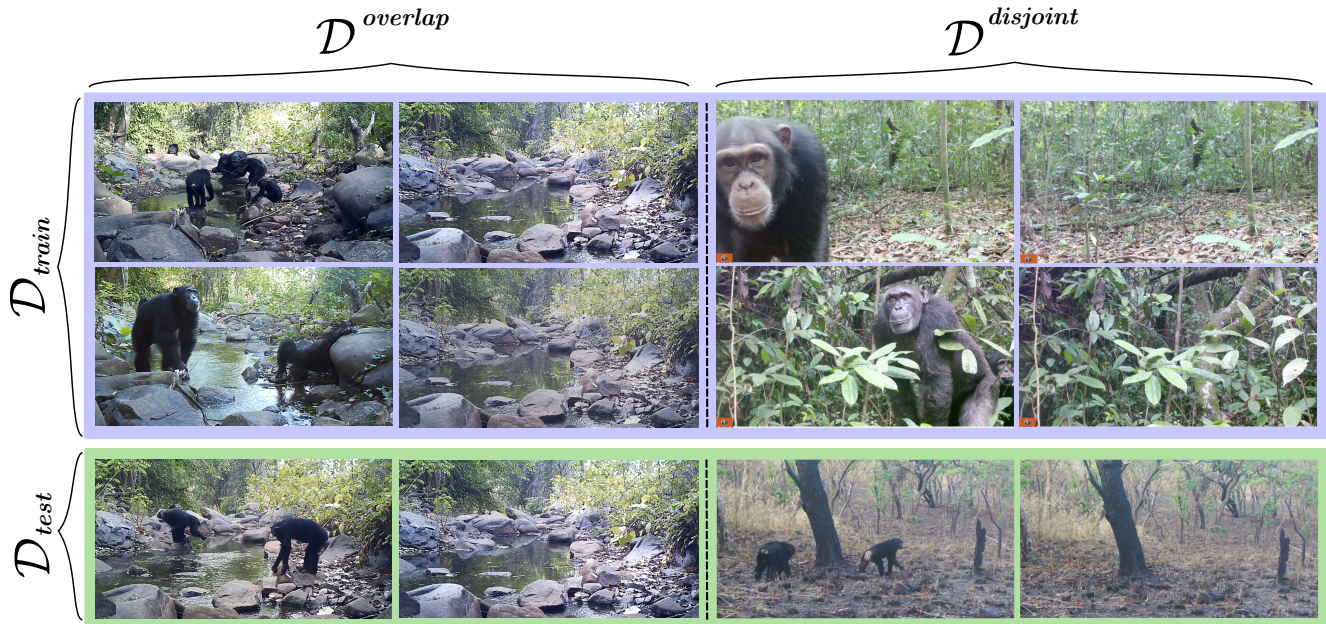


Figure 4. **Overlapping & Disjoint Dataset Configurations.** Six foreground-background video pairs are shown to visualise overlapping (left) and disjoint (right) dataset configurations. On the left, train and test videos taken from the same camera are selected, emphasizing that the locations are not mutually exclusive, with backgrounds containing several cues that are highly correlated with the displayed behaviours (i.e., algae fishing, a form of tool use). Train and test videos on the right are extracted from mutually exclusive or *disjoint* camera locations. They are extracted from forest and savannah, respectively, and highlight the challenge of generalising to new locations.

5.2. Background Reliance

Experimental Overview. First, we examined the reliance of animal behaviour recognition on the background by training model architectures on the foreground \mathcal{F} , background \mathcal{B} , and synthetic background videos $\tilde{\mathcal{B}}$ only. We refer to models trained on \mathcal{F} and \mathcal{B} (or $\tilde{\mathcal{B}}$) as FG-only and BG-only models, respectively, as shown earlier in Fig. 1. To separate background information from class-distribution intrinsic information, a dummy classifier with no access to visual information was also evaluated. It would effectively return predictions based on the class distribution information alone. Since our dataset consists of unique foreground-background pairs, it was possible to train BG-only models by retaining the original labels associated with the foreground video of the pairing. In all cases, models were tested on \mathcal{F} for comparability. Note that this makes the task more difficult for BG-only models, since animals are only observed at test time and not during training. All experiments are conducted on both $D^{overlap}$ as well as $D^{disjoint}$.

Dual-Stream Fusion Model ($\mathcal{F}+\mathcal{B}$). To clarify whether BG-only models and FG-only models, each trained separately, can be fused late to orthogonally contribute towards performance we also implemented a dual-stream model. To do this, the independently optimised weights of the FG-only and BG-only models trained for 300 epochs were loaded. During training the weights were frozen and video pairs

were processed to extract late features z^F and z^B . For ResNet models, features were extracted from the last convolutional layer and in MViT-V2 models an average of the tokens from the last hidden state were taken. Late features were then concatenated $\tilde{z} = [z^F, z^B]$ and final class predictions were produced by a trainable multi-layer perceptron.

Result 1 – Backgrounds are a Predictor of Animal Behaviour. Table 1 shows that BG-only models achieve strong performance when compared to their respective FG-only counterparts. To most clearly illustrate this, the ratio of background-to-foreground performance $\frac{AP^B}{AP^F}$ published in [8] is reported for each architecture in rows 6, 11, and 16. Background-to-foreground performance ratios are consistently high across all models, never dropping below 70% and 65% for uAP and mAP, respectively, on either dataset. This indicates that much of the behaviour recognition performance is *indeed* achievable by just utilisation of background information - the environment is a strong predictor of behaviour, even out-of-distribution. Thus, features of the environment are already behaviour predictors (trees for climbing, paths for travel, termite mound for feeding etc.). This result is further confounded by the fact that BG-only models outperform the non-visual classifier (row 1) by a significant margin, particularly on $D^{overlap}$. On $D^{disjoint}$ this observation still holds, although by somewhat smaller margins. Note that for the weakest model (2D R50) back-

Model	Data	$\mathcal{D}^{overlap}$		$\mathcal{D}^{disjoint}$		
		uAP	mAP	uAP	mAP	
1	Dummy	-	19.15	14.73	19.61	14.87
2	2D R50	\mathcal{F}	64.15	41.28	44.67	18.08
3		\mathcal{B}	57.13	30.03	45.80	18.27
4		$\tilde{\mathcal{B}}$	57.87	30.82	48.28	20.39
5		$\mathcal{F} + \mathcal{B}$	67.74	44.99	45.28	18.84
6			89.06	74.67	102.53	98.94
7	3D R50	\mathcal{F}	72.79	49.32	57.74	30.89
8		\mathcal{B}	58.92	31.72	48.40	21.38
9		$\tilde{\mathcal{B}}$	59.60	32.86	49.29	21.64
10		$\mathcal{F} + \mathcal{B}$	76.41	53.57	65.66	39.17
11			80.95	66.63	83.82	69.21
12		\mathcal{F}	75.44	51.54	70.50	35.29
13	MViT-V2	\mathcal{B}	61.90	32.74	50.03	24.00
14		$\tilde{\mathcal{B}}$	62.15	33.58	52.13	24.77
15		$\mathcal{F} + \mathcal{B}$	72.82	53.49	68.00	38.09
16			82.05	65.15	70.96	68.00

Table 1. **Quantifying Background Reliance.** Performance comparison of models trained on \mathcal{F} , \mathcal{B} , and $\tilde{\mathcal{B}}$ videos. Dual-stream models are indicated by $\mathcal{F} + \mathcal{B}$. The absolute highest performance is indicated in **bold** whereas best performance using only a single-stream is underlined. The performance based on class distribution only is given by a dummy classifier (see row 1). The background-to-foreground performance ratio is also provided (see rows 6, 11, and 16). Performance is reported on $\mathcal{D}^{overlap}$ and $\mathcal{D}^{disjoint}$ where Fig. 1 visualises an mAP scatter plot between the two for 3D R50.

ground mAP is even on-par or above the foreground baseline (see rows 2-3 in the final column). Together, these results illustrate powerfully, that across architectures background information alone is employable as a strong animal behaviour predictor.

Result 2 – Transformers rely less on Backgrounds. On the overlapping dataset, the 3D-R50 and MViT-V2 models (rows 7-16) display significantly better performance when compared with the 2D-R50 (rows 2-6), and perform similarly to each other with respect to uAP and mAP. However, the MViT-V2 model widely outperforms the 3D R50 on the disjoint dataset, suggesting that it does not rely as heavily on background features for performance. In support of this, while all models experience a large decrease in performance when moving from the overlapping to the disjoint dataset (generalisation gap), the smallest impact is on the MViT-V2. These differences between architectures are highlighted most clearly by observing uAP on the disjoint dataset. Here, the background only ratio for the MViT-V2 model is $\sim 30\%$ and $\sim 13\%$ lower than the 2D-R50 and 3D-R50, respectively. MViT-V2 achieves the best overall performance and exhibits the lowest background-to-foreground performance ratio on both dataset configurations, corroborating similar findings from the still image do-

main that show transformers are more invariant to changes in the background [34].

Analysing Background Information Contributions.

The dual 3D-R50 model achieves significant performance gains over its FG-only baseline, particularly on $\mathcal{D}^{disjoint}$, where increases of 7.92% and 8.28% in uAP and mAP, respectively, can be observed. Smaller, but still significant improvements are also observed on $\mathcal{D}^{overlap}$ (+3.62% uAP and +4.25% mAP). Interestingly, the performance of the dual-stream 3D-R50 exceeds that of MViT-v2, including its dual-stream counterpart, on nearly all metrics except for disjoint uAP. The dual-stream MViT-V2 model, on the other hand, shows improved mAP but a lower uAP when compared with the baseline model, a trend consistent across both dataset configurations. This analysis indicates that BG-only performance in the wildlife domain is *not* a subset of the FG-only model – which of course also has access to background information. Instead, explicitly learned (and frozen) background features can aid the FG-only baseline in models such as ResNet via late fusion. Finally, all BG-only models trained on $\tilde{\mathcal{B}}$ seem to outperform those trained on \mathcal{B} . However, we will show later in Sec. 5.4 that non-synthetic background videos dominate synthetic counterparts when explicitly utilised for performance improvements above the foreground baselines.

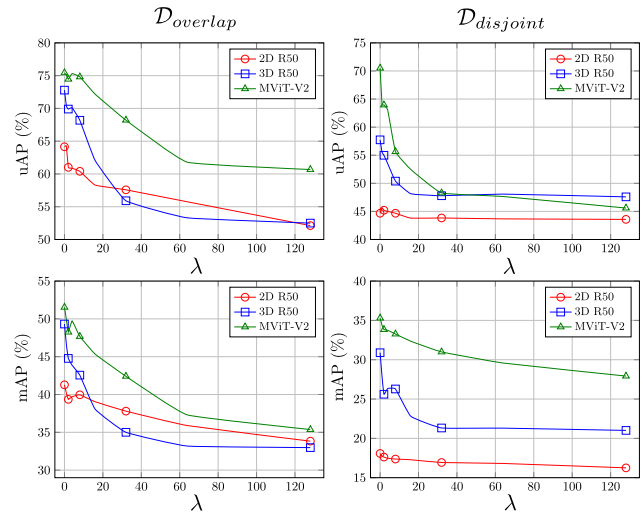


Figure 5. **The Effect of increasing Background Duration on Micro- and Mean- Average Precision.** Comparison of 2D R50, 3D R50 and MViT-V2 model performance as a function of the simulated background duration (λ). The 3D-R50 is more sensitive to increasing background durations than MViT-V2. MViT-V2 is relatively robust to increasing background durations on the overlapping dataset, although it becomes highly sensitive when evaluated on OOD data.

5.3. Background Duration

Experimental Overview. Noting that foreground videos may contain some frames with no animals, effectively supplying background only information for these frames, we aim at quantifying the effect of this on model performance (see Fig. 5). Practically, this is achieved by concatenating increasing numbers of background frames to our foreground videos. To do this, we sampled a set of λT frames from v^B , where λ is a predefined factor controlling the proportion of background frames used. The sampled background frames are denoted as $V^B = \{V_{i_0}^B, V_{i_1}^B, \dots, V_{i_{\lambda T-1}}^B\}$, with each index i_j selected from $\{0, \dots, T-1\}$. The foreground frames $V^F = \{F_0^F, F_1^F, \dots, F_{T-1}^F\}$ were then concatenated with V^B , resulting in a combined video sequence $V^{\text{concat}} = \{F_0^F, F_1^F, \dots, F_{T-1}^F, F_{i_0}^B, F_{i_1}^B, \dots, F_{i_{\lambda T-1}}^B\}$ of length $T + \lambda T$. From this concatenated sequence, a starting frame F_{start} was sampled at random from the indices $\{0, \dots, \lambda T\}$, ensuring that T consecutive frames could be sampled without exceeding the sequence bounds. The final sampled frame sequence $S = \{F_{\text{start}}, F_{\text{start}+1}, \dots, F_{\text{start}+T-1}\}$ was then used as input for training while retaining the original label y from the foreground video v^F .

Analysing the Continuum Between Foreground and Background Videos. Figure 5 shows the full performance comparison between the 2D R50, 3D R50 and MViT-V2 models as background duration increases in videos (λ). As expected, Figure 5 confirms that as λ increases model performance declines towards background model performance (see Tab 1). On $\mathcal{D}^{\text{overlap}}$, the 3D-R50 and MViT-V2 models exhibit a sharp decline before beginning to converge. This occurs at $\lambda = 32$ and $\lambda = 64$ for the 3D-R50 and MViT-V2 models, respectively. Additionally, as shown by the interval between $\lambda = 0$ and $\lambda = 32$, the uAP and mAP of 3D-R50 falls by 16.88% and 14.32%, respectively, while falling by only 7.23% and 9.13% for the MViT-V2 model. Earlier convergence to near BG-only performance and a more rapid rate of decline, show that 3D-R50 is more sensitive to increases in background durations than MViT-V2. Despite starting from lower performance, the 2D R50 model exhibits a more gradual, near-linear decline, indicating less sensitivity to changes in λ . While the behaviour of the 2D-R50 and 3D-R50 models remain relatively consistent on $\mathcal{D}^{\text{disjoint}}$, the behaviour of MViT-V2 changes significantly. Its uAP declines more steeply, falling from 70.05% to 48.29% (a decrease of 22.21%) between $\lambda = 0$ and $\lambda = 32$, where its performance converges. It is also more sensitive to smaller increases in background durations, falling from 70.50% to 64.08% (a decrease of 6.42%) between $\lambda = 0$ and $\lambda = 1.0$, where a decrease of only 0.38% is experienced on $\mathcal{D}^{\text{overlap}}$ over the same interval. At higher values of λ (i.e., > 40) the performance drops below that of the 3D-R50 (although only once

the background-only performance has been surpassed). Although uAP falls more steeply, mAP declines more slowly and performance above that of the BG-only model is maintained even at the highest values of λ . This suggests that, although the MViT-V2 achieves higher baseline performance on the disjoint dataset, it is more sensitive to increases in background frames when evaluating uAP – a specific data scenario drowning the advantages of the transformer model in background information.

5.4. Background Bias Mitigation

Augmenting Performance via Explicit Background Neutralisation. In this final experimental section, we justify the need for paired, real-world background samples, as uniquely provided by our dataset. We show that these sample pairings are demonstrably qualified to significantly improve model performance. To show this, we analyse the impact of background subtraction operations in both input and embedding spaces across each of the model architectures and dataset configurations. Two background-subtracted views of our dataset were created for input space experiments. This was done by performing pixel-wise subtraction of \mathcal{B} and $\tilde{\mathcal{B}}$ from \mathcal{F} . To perform algebraic background subtraction in latent space, we extracted the feature vectors of the foreground video pairs. As described in Sec. 5.2, we achieve this by processing the video tensors up to the last convolutional layer and averaging the tokens from the last hidden state in the ResNet and MViT-V2 models, respectively. The background-subtracted embedding is then computed as $z^{\mathcal{F}-\mathcal{B}} = z^{\mathcal{F}} - (1 - \alpha) \cdot z^{\mathcal{B}}$ where α is a coefficient used to control the relative magnitude of the algebraic subtraction operation as schematically shown in Fig. 6. In practice, the modulation parameter $\alpha \in [0, 1]$ was ablated to increase linearly or exponentially over the course of training and results are reported for both. In all cases α was initialized at zero and increased to one by the end of training.

Results and Performance Improvements. For the basic 2D-R50 model, background subtraction in input space is highly effective. When using \mathcal{B} , we observe substantial performance improvements over the baseline, with percentage increases of +8.06% and 5.84% in uAP and mAP on $\mathcal{D}^{\text{overlap}}$, and +9.06% and +7.76% in uAP and mAP on $\mathcal{D}^{\text{disjoint}}$. Using $\tilde{\mathcal{B}}$ also yields improvements, though these gains are notably smaller. Background subtraction in embedding space does not provide any benefit to the 2D-R50. Although input space background subtraction is effective for the 2D-R50, it does not improve performance for the 3D-R50 and MViT-V2 models. Neither original nor synthetic backgrounds provide an advantage over their respective baselines, indicating that input space subtraction may not be suitable for architectures that process spatio-temporal features.

Model	Subtraction	$\mathcal{D}^{overlap}$		$\mathcal{D}^{disjoint}$	
		u	m	u	m
2D R50	Baseline	64.15	41.28	44.67	18.08
	$\mathcal{F} - \tilde{\mathcal{B}}$	65.96	42.12	54.53	26.65
	$\mathcal{F} - \mathcal{B}$	72.21	47.12	53.73	25.84
	None	56.21	38.84	27.24	17.94
	Linear	53.78	39.01	29.75	17.17
	Exponential	54.05	37.11	25.80	17.73
3D R50	Baseline	72.79	49.32	57.74	30.89
	$\mathcal{F} - \tilde{\mathcal{B}}$	66.51	42.56	53.58	27.98
	$\mathcal{F} - \mathcal{B}$	71.93	46.36	53.92	25.05
	None	72.30	51.39	63.14	34.85
	Linear	77.31	52.82	66.69	36.31
	Exponential	73.52	51.24	64.58	36.36
MViT-V2	Baseline	75.44	51.54	70.50	35.29
	$\mathcal{F} - \tilde{\mathcal{B}}$	66.84	42.27	57.21	28.80
	$\mathcal{F} - \mathcal{B}$	74.90	49.40	61.22	31.51
	None	74.23	44.11	68.56	35.14
	Linear	79.32	53.83	71.64	39.04
	Exponential	77.70	50.93	71.28	39.25

Table 2. **Quantifying Performance Improvements of Background Subtraction.** Performance comparison of the 2D R50, 3D R50, and MViT-V2 models on both dataset configurations: \mathcal{D}_O and \mathcal{D}_D . Each model’s performance is reported when training on $\mathcal{F} - \mathcal{B}$ or $\mathcal{F} - \tilde{\mathcal{B}}$ videos in input (light green) and embedding space (light blue). The highest scores are indicated in **bold**. Results confirm superiority of the availability of paired, real-world background videos and algebraic operation in embedding space, that is over synthetic data or input space operations.

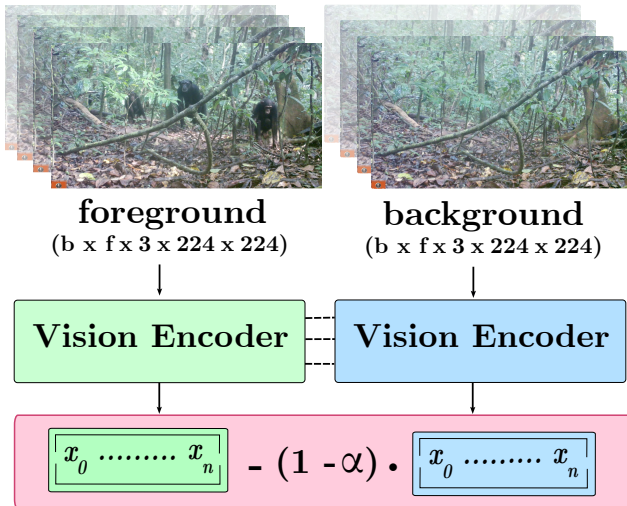


Figure 6. **Latent Space Background Compensation.** The proposed operation uses α to perform a weighted subtraction of background features (computed via the dataset pairing of a real-world, background video) from foreground features in latent space. The dotted line between the encoders indicates shared weights (i.e., they are the same model).

Conversely, background subtraction in embedding space provides significant performance improvements for the 3D-R50 and MViT-V2 models, particularly on $\mathcal{D}^{disjoint}$. For the 3D-R50, embedding space subtraction with linear scheduling results in a +8.95% and +5.42% increase in uAP and mAP, respectively. Exponential scheduling also yields improvements over the baseline. The improvements are lower than linear scheduling with respect to uAP (+6.84%) but marginally better for mAP (+5.47%). MViT-V2 also benefits from embedding space subtraction on $\mathcal{D}^{disjoint}$: linear scheduling improves uAP and mAP by +1.14% and +3.75%, respectively, whereas exponential scheduling provides a +0.78% increase in uAP and a +3.96% increase in mAP. These findings suggest that embedding space subtraction is effective for both 3D-R50 and MViT-V2 models on $\mathcal{D}^{disjoint}$, with linear and exponential scheduling favouring uAP and mAP performance, respectively. Embedding space subtraction also enhances performance on $\mathcal{D}^{overlap}$, though to a lesser extent than on $\mathcal{D}^{disjoint}$. For the 3D-R50 model, applying embedding space subtraction with linear scheduling yields an improvement of 4.52% and 3.50% in uAP and mAP, respectively, while exponential scheduling results in smaller gains of 0.73% and 1.92%. The MViT-V2 model follows a similar trend: linear scheduling increases uAP and mAP by 3.88% and 2.29%, respectively, whereas exponential scheduling improves uAP by 2.26% but slightly reduces mAP by -0.61%. These results suggest that algebraic embedding space subtraction is beneficial on $\mathcal{D}^{overlap}$, although the performance gains are relatively small compared to $\mathcal{D}^{disjoint}$, and that linear scheduling generally provides better results than exponential scheduling.

6. Limitations

Key limitations include that; (1) our experiments and dataset relate, due to the nature of camera traps, to statically installed sensors only; (2) the latent space background subtraction requires additional data (in the form of background frames) and has computational implications of two forward passes of the model (instead of one) for each training step; (3) the background concatenation experiments may have synthesised videos that are unnatural (e.g., a chimpanzee sitting could suddenly disappear without moving out of frame) and may affect learning performance.

7. Conclusion

In this work, we introduced PanAf-FGBG – the first wildlife dataset specifically designed to evaluate backgrounds and out-of-distribution generalisation for behaviour recognition. It is a large, richly annotated wild chimpanzee behaviour dataset which defines explicit data configurations for experiments with overlapping and disjoint camera locations. Performing in-depth experimentation with this unique dataset,

we demonstrated that real-world background information from wild habitats is not only a powerful predictor of animal behaviour, but can be utilised to significantly improve recognition performance across models.

Beyond these results, the release of this dataset will enable the computer vision community to run direct evaluative studies under in-distribution and out-of-distribution conditions to improve the utilisation of backgrounds for deep action recognition in the wildlife domain. The rich metadata will allow further tasks and experimental configurations to be created. We hope that this will aid model transferability and performance in this challenging domain and ultimately benefit endangered and charismatic species like the one featured in this paper.

Supplementary Material

In the supplementary material, we provide: (i) additional dataset statistics in Sec. 1; (ii) a description of how synthetic background videos are created in Sec. 2; (iii) foreground-background video pair visualisations (see Fig 5) and; (iv) a visualisation showcasing a small fraction ($\sim 0.05\%$) of the total available frames (see Fig. 6)

1. Dataset Statistics

We present additional dataset statistics for the country, research site, camera locations and behaviours. Specifically, (i) the distribution of countries and the corresponding research sites are displayed in Fig. 1 (ii) the accumulative proportion of videos contributed by each camera is shown in Fig. 2 and; (iii) a comparison of the behaviour distribution for the overlapping and disjoint datasets is displayed in Fig. 3

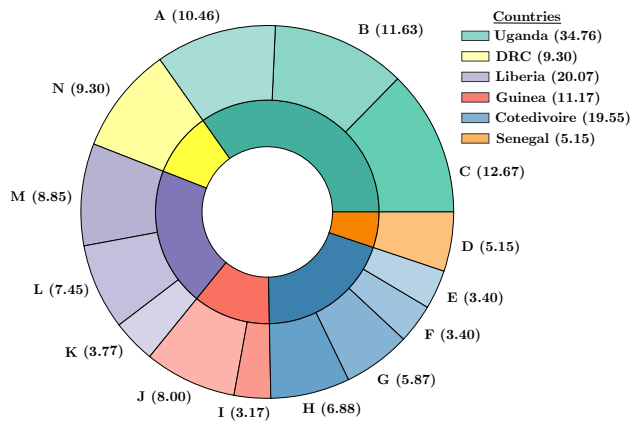


Figure 1. **Proportion of videos from each country and research site.** The inner ring displays the proportion of videos extracted from each country, while the outer ring represents individual research sites. Each research site segment is a unique shade derived from its corresponding country’s colour. All proportions are shown in brackets. Note that research site names are replaced with letters to protect the location of the chimps.

2. Synthetic Background Generation

We generated synthetic background videos using SAM2 [37] and mean pixel value filling. Specifically, we prompted the SAM2.1-Large model using a single spatial coordinate indicating the location of the chimpanzee to produce an initial segmentation mask. We then leveraged the automatic mask propagation functionality of SAM2 to create spatio-temporal masklets for the full video. Note that spatial coordinates were produced manually. Then, we

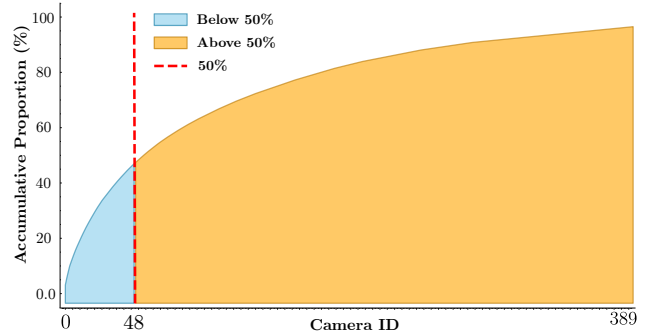


Figure 2. **Accumulative proportion of videos contributed by each camera.** The y-axis represents the accumulative proportion of videos, with individual cameras arranged by their contribution on the x-axis. The red dashed line divides the cameras into two groups: those contributing the first 50% of the data (left) and the remaining 50% (right). Many videos are contributed by a relatively small number of cameras: 48 cameras contribute 50% of the footage.

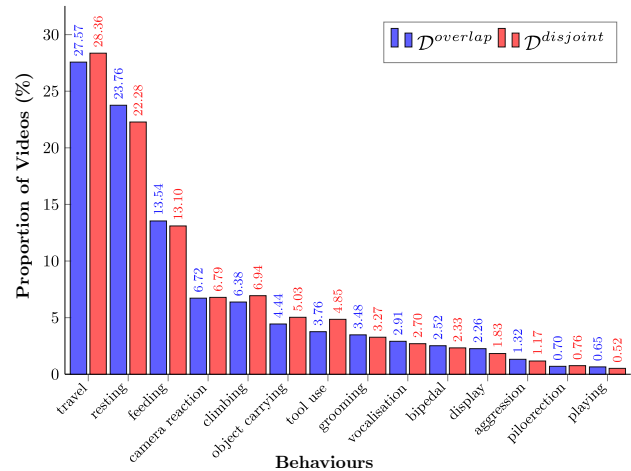


Figure 3. **Comparison of the proportion of videos containing each behaviour between overlapping and disjoint datasets.** Proportions for the overlapping dataset are shown in blue and the disjoint dataset in red. Behaviours are ordered from highest to lowest proportion, with exact values displayed above each bar for easy comparison.

filled the area indicated by the segmentation mask with the mean pixel value for the frame (see Fig. 4 for examples). Synthetic background videos, spatial coordinates, and segmentation masks will be published with the dataset.



Figure 4. **Synthetic Background Video Examples.** Three example video clips with the original segmentation mask generated by one-shot prompting of SAM2 overlaid and the corresponding mean pixel value filled frame.



Figure 5. **Foreground-Background Video Pair Examples.** Shown are 18 pairs of still frames (two pairs per row) extracted from foreground-background video pairs.



Figure 6. **Dataset Overview.** A small fraction ($\sim 0.05\%$) of the 1.8 million frames in the dataset are shown, highlighting its diversity with respect to exhibited behaviours, habitat, weather conditions, time of day, and more.

References

- [1] Pan African Programme: The Cultured Chimpanzee, 1999. Online; accessed 29 January 2014. [3](#)
- [2] Mimi Arandjelovic, Colleen R Stephens, Maureen S McCarthy, Paula Dieguez, Ammie K Kalan, Nuria Maldonado, Christophe Boesch, and Hjalmar S Kuehl. Chimp&see: An online citizen science platform for large-scale, remote video camera trap annotation of chimpanzee behaviour, demography and individual identification. *PeerJ Preprints*, 2016. [4](#)
- [3] Sara Beery, Arushi Agarwal, Elijah Cole, and Vighnesh Birodkar. The iwildcam 2021 competition dataset. *arXiv preprint arXiv:2105.03494*, 2021. [3](#)
- [4] Otto Brookes, Majid Mirmehdi, Colleen Stephens, Samuel Angedakin, Katherine Corogenes, Dervla Dowd, Paula Dieguez, Thurston C Hicks, Sorrel Jones, Kevin Lee, et al. Panaf20k: a large video dataset for wild ape detection and behaviour recognition. *International Journal of Computer Vision*, pages 1–17, 2024. [2](#), [3](#)
- [5] Jackie Chappell and Susannah KS Thorpe. The role of great ape behavioral ecology in one health: Implications for captive welfare and re-habilitation success. *American journal of primatology*, 84(4-5):e23328, 2022. [2](#)
- [6] Jun Chen, Ming Hu, Darren J Coker, Michael L Berumen, Blair Costelloe, Sara Beery, Anna Rohrbach, and Mohamed Elhoseiny. Mammalnet: A large-scale video benchmark for mammal recognition and behavior understanding. In *Proceedings of the IEEE/CVF conference on computer vision and pattern recognition*, pages 13052–13061, 2023. [2](#), [3](#)
- [7] Jinwoo Choi, Chen Gao, Joseph CE Messou, and Jia-Bin Huang. Why can't i dance in the mall? learning to mitigate scene bias in action recognition. *Advances in Neural Information Processing Systems*, 32, 2019. [1](#), [3](#), [4](#)
- [8] Jihoon Chung, Yu Wu, and Olga Russakovsky. Enabling detailed action recognition evaluation through video dataset augmentation. *Advances in Neural Information Processing Systems*, 35:39020–39033, 2022. [1](#), [3](#), [4](#), [5](#)
- [9] Fay E Clark. Great ape cognition and captive care: Can cognitive challenges enhance well-being? *Applied Animal Behaviour Science*, 135(1-2):1–12, 2011. [2](#)
- [10] Fagner Cunha, Eulanda M dos Santos, Raimundo Barreto, and Juan G Colonna. Filtering empty camera trap images in embedded systems. In *Proceedings of the IEEE/CVF Conference on Computer Vision and Pattern Recognition*, pages 2438–2446, 2021. [2](#)
- [11] Alexander D'Amour, Katherine Heller, Dan Moldovan, Ben Adlam, Babak Alipanahi, Alex Beutel, Christina Chen, Jonathan Deaton, Jacob Eisenstein, Matthew D Hoffman, et al. Underspecification presents challenges for credibility in modern machine learning. *Journal of Machine Learning Research*, 23(226):1–61, 2022. [1](#)
- [12] Shuangrui Ding, Maomao Li, Tianyu Yang, Rui Qian, Hao-hang Xu, Qingyi Chen, Jue Wang, and Hongkai Xiong. Motion-aware contrastive video representation learning via foreground-background merging. In *Proceedings of the IEEE/CVF conference on computer vision and pattern recognition*, pages 9716–9726, 2022. [3](#)
- [13] Isla Duporge, Maksim Kholiavchenko, Roi Harel, Dan Rubenstein, Meg Crofoot, Tanya Berger-Wolf, Stephen Lee, Scott Wolf, Julie Barreau, Jenna Kline, et al. Baboonland dataset: Tracking primates in the wild and automating behaviour recognition from drone videos. *arXiv preprint arXiv:2405.17698*, 2024. [2](#)
- [14] Robert Geirhos, Jörn-Henrik Jacobsen, Claudio Michaelis, Richard Zemel, Wieland Brendel, Matthias Bethge, and Felix A Wichmann. Shortcut learning in deep neural networks. *Nature Machine Intelligence*, 2(11):665–673, 2020. [1](#)
- [15] Rohit Girdhar and Deva Ramanan. Cater: A diagnostic dataset for compositional actions and temporal reasoning. *arXiv preprint arXiv:1910.04744*, 2019. [3](#)
- [16] Abhinav Gupta and Larry S Davis. Objects in action: An approach for combining action understanding and object perception. pages 1–8. IEEE, 2007. [3](#)
- [17] Kaiming He, Xiangyu Zhang, Shaoqing Ren, and Jian Sun. Deep residual learning for image recognition. In *Proceedings of the IEEE conference on computer vision and pattern recognition*, pages 770–778, 2016. [4](#)
- [18] Yun He, Soma Shirakabe, Yutaka Satoh, and Hirokatsu Kataoka. Human action recognition without human. In *Computer Vision—ECCV 2016 Workshops: Amsterdam, The Netherlands, October 8-10 and 15-16, 2016, Proceedings, Part III 14*, pages 11–17. Springer, 2016. [1](#), [2](#), [3](#)
- [19] Lisa Anne Hendricks, Kaylee Burns, Kate Saenko, Trevor Darrell, and Anna Rohrbach. Women also snowboard: Overcoming bias in captioning models. In *Proceedings of the European conference on computer vision (ECCV)*, pages 771–787, 2018. [1](#), [4](#)
- [20] Filip Ilic, Thomas Pock, and Richard P Wildes. Is appearance free action recognition possible? In *European Conference on Computer Vision*, pages 156–173. Springer, 2022. [1](#), [3](#)
- [21] Will Kay, Joao Carreira, Karen Simonyan, Brian Zhang, Chloe Hillier, Sudheendra Vijayanarasimhan, Fabio Viola, Tim Green, Trevor Back, Paul Natsev, et al. The kinetics human action video dataset. *arXiv preprint arXiv:1705.06950*, 2017. [4](#)
- [22] Maksim Kholiavchenko, Jenna Kline, Michelle Ramirez, Sam Stevens, Alec Sheets, Reshma Babu, Namrata Banerji, Elizabeth Campolongo, Matthew Thompson, Nina Van Tiel, et al. Kabr: In-situ dataset for kenyan animal behavior recognition from drone videos. In *Proceedings of the IEEE/CVF Winter Conference on Applications of Computer Vision*, pages 31–40, 2024. [2](#)
- [23] Pang Wei Koh, Shiori Sagawa, Henrik Marklund, Sang Michael Xie, Marvin Zhang, Akshay Balsubramani, Weihua Hu, Michihiro Yasunaga, Richard Lanus Phillips, Irena Gao, et al. Wilds: A benchmark of in-the-wild distribution shifts. In *International conference on machine learning*, pages 5637–5664. PMLR, 2021. [1](#), [3](#), [4](#)
- [24] Hjalmar S Kühl and Tilo Burghardt. Animal biometrics: quantifying and detecting phenotypic appearance. *Trends in ecology & evolution*, 28(7):432–441, 2013. [1](#)
- [25] Haoxin Li, Yuan Liu, Hanwang Zhang, and Boyang Li. Mitigating and evaluating static bias of action representations in

- the background and the foreground. In *Proceedings of the IEEE/CVF International Conference on Computer Vision*, pages 19911–19923, 2023. 1, 3
- [26] Yi Li and Nuno Vasconcelos. Repair: Removing representation bias by dataset resampling. In *Proceedings of the IEEE/CVF conference on computer vision and pattern recognition*, pages 9572–9581, 2019. 1, 3
- [27] Yingwei Li, Yi Li, and Nuno Vasconcelos. Resound: Towards action recognition without representation bias. In *Proceedings of the European Conference on Computer Vision (ECCV)*, pages 513–528, 2018. 3
- [28] Yanghao Li, Chao-Yuan Wu, Haoqi Fan, Karttikeya Mangalam, Bo Xiong, Jitendra Malik, and Christoph Feichtenhofer. Mvitv2: Improved multiscale vision transformers for classification and detection. In *Proceedings of the IEEE/CVF conference on computer vision and pattern recognition*, pages 4804–4814, 2022. 4
- [29] Dan Liu, Jin Hou, Shaoli Huang, Jing Liu, Yuxin He, Bochuan Zheng, Jifeng Ning, and Jingdong Zhang. Lote-animal: A long time-span dataset for endangered animal behavior understanding. In *Proceedings of the IEEE/CVF International Conference on Computer Vision*, pages 20064–20075, 2023. 2, 3
- [30] I Loshchilov. Decoupled weight decay regularization. *arXiv preprint arXiv:1711.05101*, 2017. 4
- [31] Xiaoxuan Ma, Stephan Kaufhold, Jiajun Su, Wentao Zhu, Jack Terwilliger, Andres Meza, Yixin Zhu, Federico Rossano, and Yizhou Wang. Chimpact: A longitudinal dataset for understanding chimpanzee behaviors. *Advances in Neural Information Processing Systems*, 36:27501–27531, 2023. 2, 3
- [32] Marcin Marszałek, Ivan Laptev, and Cordelia Schmid. Actions in context. In *2009 IEEE Conference on Computer Vision and Pattern Recognition*, pages 2929–2936. IEEE, 2009. 2, 3
- [33] Zhongqi Miao, Ziwei Liu, Kaitlyn M Gaynor, Meredith S Palmer, Stella X Yu, and Wayne M Getz. Iterative human and automated identification of wildlife images. *Nature Machine Intelligence*, 3(10):885–895, 2021. 2
- [34] Mazda Moayeri, Phillip Pope, Yogesh Balaji, and Soheil Feizi. A comprehensive study of image classification model sensitivity to foregrounds, backgrounds, and visual attributes. In *Proceedings of the IEEE/CVF Conference on Computer Vision and Pattern Recognition*, pages 19087–19097, 2022. 2, 6
- [35] Xun Long Ng, Kian Eng Ong, Qichen Zheng, Yun Ni, Si Yong Yeo, and Jun Liu. Animal kingdom: A large and diverse dataset for animal behavior understanding. In *Proceedings of the IEEE/CVF conference on computer vision and pattern recognition*, pages 19023–19034, 2022. 2, 3
- [36] Joaquin Quiñero-Candela, Masashi Sugiyama, Anton Schwaighofer, and Neil D Lawrence. *Dataset shift in machine learning*. Mit Press, 2022. 1
- [37] Nikhila Ravi, Valentin Gabeur, Yuan-Ting Hu, Ronghang Hu, Chaitanya Ryali, Tengyu Ma, Haitham Khedr, Roman Rädle, Chloe Rolland, Laura Gustafson, et al. Sam 2: Segment anything in images and videos. *arXiv preprint arXiv:2408.00714*, 2024. 4, 1
- [38] Herbert Robbins and Sutton Monro. A stochastic approximation method. *The annals of mathematical statistics*, pages 400–407, 1951. 4
- [39] Vaishaal Shankar, Achal Dave, Rebecca Roelofs, Deva Ramanan, Benjamin Recht, and Ludwig Schmidt. Do image classifiers generalize across time? In *Proceedings of the IEEE/CVF International Conference on Computer Vision*, pages 9661–9669, 2021. 2
- [40] Devis Tuia, Benjamin Kellenberger, Sara Beery, Blair R Costelloe, Silvia Zuffi, Benjamin Risse, Alexander Mathis, Mackenzie W Mathis, Frank Van Langevelde, Tilo Burghardt, et al. Perspectives in machine learning for wildlife conservation. *Nature communications*, 13(1):1–15, 2022. 1
- [41] Tuan-Hung Vu, Catherine Olsson, Ivan Laptev, Aude Oliva, and Josef Sivic. Predicting actions from static scenes. In *Computer Vision—ECCV 2014: 13th European Conference, Zurich, Switzerland, September 6–12, 2014, Proceedings, Part V 13*, pages 421–436. Springer, 2014. 1, 2, 3
- [42] Jinpeng Wang, Yuting Gao, Ke Li, Yiqi Lin, Andy J Ma, Hao Cheng, Pai Peng, Feiyue Huang, Rongrong Ji, and Xing Sun. Removing the background by adding the background: Towards background robust self-supervised video representation learning. In *Proceedings of the IEEE/CVF conference on computer vision and pattern recognition*, pages 11804–11813, 2021. 3
- [43] Kai Xiao, Logan Engstrom, Andrew Ilyas, and Aleksander Madry. Noise or signal: The role of image backgrounds in object recognition. *arXiv preprint arXiv:2006.09994*, 2020. 3
- [44] Manlin Zhang, Jinpeng Wang, and Andy J Ma. Suppressing static visual cues via normalizing flows for self-supervised video representation learning. In *Proceedings of the AAAI Conference on Artificial Intelligence*, pages 3300–3308, 2022. 3
- [45] Mingjun Zhao, Yakun Yu, Xiaoli Wang, Lei Yang, and Di Niu. Search-map-search: a frame selection paradigm for action recognition. In *Proceedings of the IEEE/CVF Conference on Computer Vision and Pattern Recognition*, pages 10627–10636, 2023. 3
- [46] Xingyi Zhou, Anurag Arnab, Chen Sun, and Cordelia Schmid. How can objects help action recognition? In *Proceedings of the IEEE/CVF Conference on Computer Vision and Pattern Recognition*, pages 2353–2362, 2023. 3
- [47] Yi Zhu, Xinyu Li, Chunhui Liu, Mohammadreza Zolfaghari, Yuanjun Xiong, Chongruo Wu, Zhi Zhang, Joseph Tighe, R Manmatha, and Mu Li. A comprehensive study of deep video action recognition. *arXiv preprint arXiv:2012.06567*, 2020. 1